Voltage Nonlinear Control in Multiterminal HVDC Networks

Luís M. C. Nunes, MSc Student, IST, J. Fernando A. Silva, Senior Member, IEEE

***Abstract*— The use of DC networks including the transmission of energy using DC current at high voltage HVDC has become a reality with the advancement of power electronics. The HVDC system, for long distances has advantages in terms of the environment, cost, weight, losses, public health when compared to the traditional HVAC, while allowing the interconnection of two independent asynchronous AC networks directly.**

The purpose of this dissertation is to model and control a standard multiterminal DC network which consists in the interconnection of two independent networks. Each of these networks have an AC source, inverter, DC-DC converter, resistive loads, and electronic loads (constant power and constant current). Two nonlinear control strategies were created including droop control. These controllers must be able to control the voltage steady state regardless of disturbances.

The developed controllers for the three-phase inverter-rectifier and for the DC-DC converters are based on two nonlinear control methods based on the theory of Lyapunov stability and combine the theory of the backstepping and the theory of sliding mode control (BSMC).

The strategy mentioned above was test in terms of response to transients and overvoltage/undervoltage through MATLAB/Simulink simulations.

***Keywords*— HVDC, HVAC, Multiterminal DC network, BSMC, Nonlinear controllers**

I. Introduction

In the last years with advancement in Electronics, especially in semiconductor technology that allowed to step-up or step-down DC voltage conversion, DC networks became a possible solution to replace or complement the AC distribution system [1].

With the recent growth in renewable energy (RE) the DC links became more interesting, because a considerable amount of RE electricity is produced using direct current. Recent studies have shown that for long distances the best way to transmit power from offshore wind farms to the coast is by high voltage direct current (HVDC) links. This fact led a new interest in the HVDC grids, especially in the study of stability and the voltage control. In this type of RE an HVDC transmission usually results in a multi-terminal network. It is possible to control this network with voltage source converters connected in its terminals (VSCs). These converters permit the transfer of the power from the DC side to AC grids where the consumers are connected. The importance of control in this multi-terminal network is to guarantee that DC voltage remains almost stable while damping out any oscillations that results from the change in the incoming power and by faults in the AC side [2].

Multi-terminal HVDC structure brings a lot of advantages such as cost maintenance and weight reduction, but also have disadvantages. The main problem is stability in DC voltage and input filters due to the presence of the constant power loads [3].

Regardless the stability issue with constant power loads, HVDC transition system is the better method to solve the problems between the interconnection of power networks, because DC power do not show frequency or phase angles incompatibilities, so it's possible to connect two separately asynchronous AC systems. For long distances HVDC system is also better because it can use underground and submarine cables. This type of system permits
more power transfer with fewer cables compared to AC system. For long distances HVAC systems have more losses than HVDC and reactive power compensation is needed and a bigger investment cost. Finally, for environment reasons HVDC is the optimal choice because it shows almost zero induction or alternating electro-magnetic fields [4].

Nonlinear controllers where developed to improve the behaviour of equipment. With nonlinear controllers such as hysteresis, sliding mode control (SMC) it is possible to control just-in time while providing a precise control action [5].

II. Modelling the Standard Multiterminal DC Network

The standard multi-terminal DC network it will be composed by two equal circuits and a third one that connects the first ones (Fig. 1). Basically, the system has two identical networks that are connected by a line that can be represented by a π model. Each network has a constant power load, current constant load and AC/DC, DC/DC converters. After obtaining the DC network model, the objective is to design nonlinear controllers able to track the DC voltage at a certain value. These controllers should also guarantee the stability of all system in a way that the all network always is stable independently of the load type in use. In addition to this the second line of the DC network will have a power controller responsible for the injection of power into to the DC grid. To conclude the description of the DC network it is also relevant to refer that both grids will have low-pass filters to attenuate the amplitude of high frequency harmonics and all strategies of control the DC voltage in inverter will have droop control.

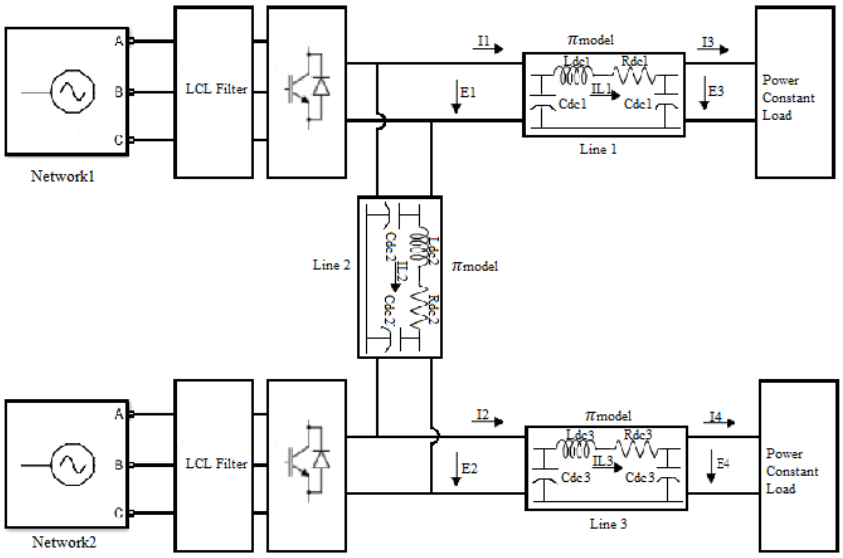

Figure 1 - Equivalent circuit of a four-terminal VSC-HVDC network with π model

A. *LCL Filter and Inverter-Rectifier*

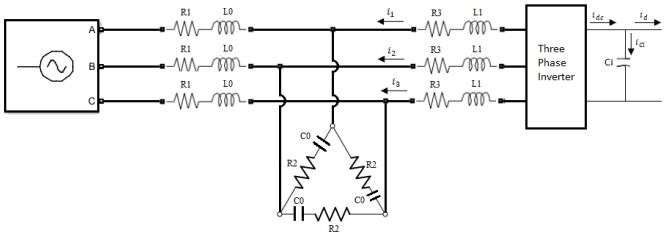

Figure 2 – LCL filter representation

For the purpose of this work the AC side powering the DC grids will be represented by a three-phase system with internal short-circuit impedance connected to a 3-phase inverter-rectifier. The AC sources short circuit resistive and inductive components of the impedances cannot be neglected due to the power levels transmitted. These sources are connected to inverter-rectifiers in the multiterminal HVDC system. The inverter-rectifier switching action injects high frequency harmonics in the current waveforms. The amplitude of the harmonics decreases with the harmonic order relative to the switching frequency but still require to be further attenuated. Therefore, in the AC side the use of a filter that acts like a low pass-filters to minimize the harmonics amplitude especially in high frequencies is required. LCL filter is going to be used instead of a traditional LC filter because presents a better performance in this type of system.

.

The operation mode of the Inverter-rectifier and the step-by-step design of the LCL filter are present in [6].

B. *HVDC Grid Configuration*

The HVDC transmission grid will be loaded by constant power loads and with DC-DC converters feeding constant current loads.

The DC-DC converter (Fig. 3) is here illustrated with a four-quadrant chopper, because this converter has three operating modes:

$$\gamma = \begin{cases} 1, & If\ S1 \wedge S4\ ON \\ 0, & \begin{cases} If\ S1 \wedge S3\ ON \\ If\ S2 \wedge S4\ ON \end{cases} \\ -1, & If\ S2 \wedge S3\ ON \end{cases} \quad (1)$$

$$V_i = \gamma U = \begin{cases} +U \\ 0 \\ -U \end{cases} \quad (2)$$

1) *Constant Current Load*

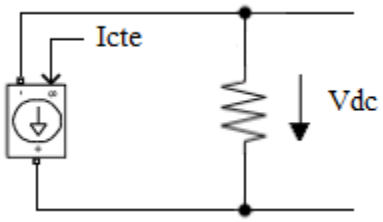

Figure 4 – Constant current load representation

From Fig. 4, supposing the load resistor is big enough to absorb negligible power, the load power P is:

$$P = V_{dc} I_{cte} \quad (3)$$

The load power P depends on the value of I_{cte} in (3).

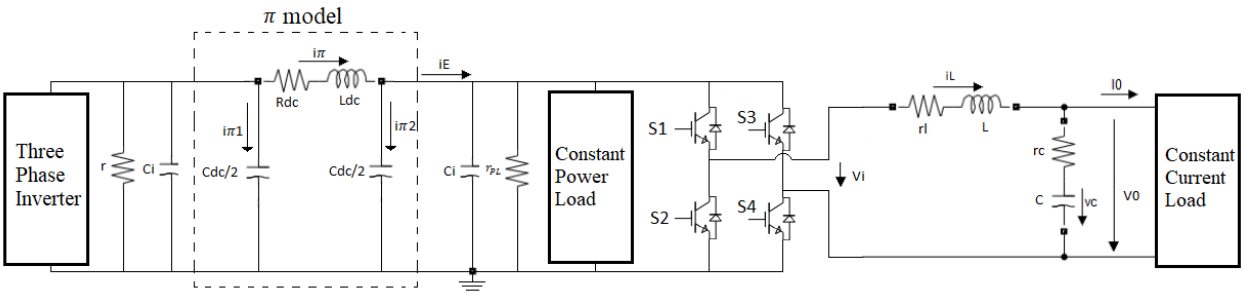

Figure 3 – HVDC transmission grid representation

2) Constant Power Load

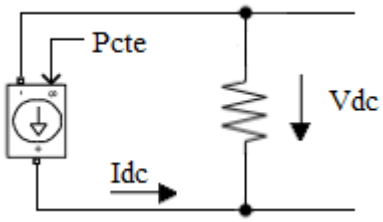

Figure 5 – Constant power load representation

From Fig. 5, supposing the represented resistor is big enough to absorb negligible power, the load constant power P is:

$$P_{cte} = I_{dc}V_{dc} = constante \tag{4}$$

For constant P_{cte}, the load current is obtained solving (4) for I_{dc}.

Constant power load exhibit negative incremental resistance (5) and this behaviour is the responsible for stability issues in transmission lines [7].

$$\frac{V_{dc}}{I_{dc}} = \frac{dV_{dc}}{dI_{dc}} = -r_{cpl} \tag{5}$$

As it shown in Fig. 6 the voltage decreases with increase in current and vice-versa. The negative impedance characteristic of constant power load is also shown.

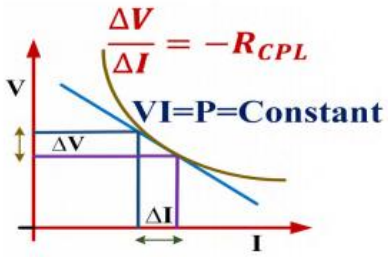

Figure 6 – V-I curve of constant power load and the negative impedance characteristic [8]

3) DC-DC Converter LC Output Filter

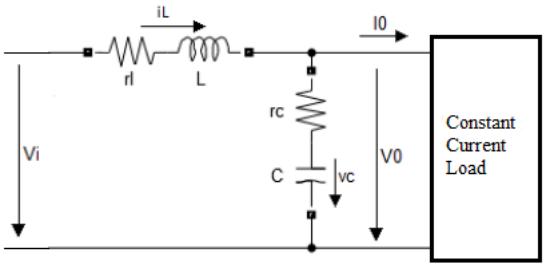

Figure 7 – LC filter

In order to have a proper LC filter the equations in the section four quadrant chopper LC filtering of [8] are used.

$$L = \frac{V_n}{4\Delta i_{Lmax}}T \tag{6}$$

$$C = \frac{V_n}{32L\Delta V_0}T^2 \tag{7}$$

Where L is the inductor filter, C is the capacitor filter, Δi_{Lmax} is the ripple of the current, V_n is the nominal DC voltage, T is the switching period, $\Delta V_0$is the voltage ripple.

III. Nonlinear Controllers

The main objective of this chapter is to design nonlinear controllers that are able to control the DC voltage and current in the inverter-rectifier and in the DC-DC converter (figures 1 and 3).

Therefore, four nonlinear controllers are going to be designed, two of them to control voltage and current in the inverter-rectifier and the other two to control the similar quantities in the DC-DC converter. Hence, to do that the direct method of Lyapunov, backstepping, and sliding mode control are the techniques to be used.

Considering the four-terminal HVDC line, and the interconnection DC line (Fig.1), to control de grid DC voltage the control strategy considers a voltage controller in thee inverter-rectifier of line 1, while in line 3 a direct power injection is assumed in the line 2 inverter-rectifier. In this way is it possible to control the grid voltage and the power

dispatched in the network. Therefore, in this chapter it will be explained the design of power and voltage controllers.

A. Inverter-Rectifier Controllers

Some techniques to design nonlinear controllers for voltage and current control have been introduced in [6]. Therefore, backstepping will be used to control the line voltage [9], while current controllers are based on sliding mode control. To control the power to be injected in line 3 (Fig.1), a power controller in dq coordinates will be introduced based on a sliding mode controller.

1) Nonlinear Voltage Controller of the Inverter-Rectifier

Considering the Fig. 2 the system model in d-q coordinates is expressed as follows:

$$\frac{du_{Ci}}{dt} = \frac{1}{C_i}\left(\frac{u_{Gi}}{u_{Ci}} i_d + i_{dc}\right) = \frac{1}{C_i}(G_i i_d + i_{dc})$$
$$\frac{di_d}{dt} = \frac{-G_i u_{Ci} - R_3 i_d + u_{Gi}}{L_1} + \omega i_q \quad (8)$$

The virtual control input is the inverter-rectifier input current d component $G_i i_d$, where $G_i = \frac{u_{Gi}}{u_{Ci}}$ is the current gain.

The control objective is defined as $u_{Ci} = u_{Ciref}$, to obtain the control law $G_i u_{Ci} = f(u_{Ciref}, u_{Ci})$.

Considering a new variable e_u, the control objective error, defined as:

$$e_u = u_{Ciref} - u_{Ci} \quad (9)$$

The purpose is to demand $e_u = 0$. To present steady-state errors add an integral of the objective error by defining:

$$e_I = \int_0^t e_u dt = 0 \quad (10)$$

According to Lyapunov the system is asymptotically stable if the candidate Lyapunov function verifies the following conditions:

$$V(x = 0) = 0$$
$$V(x \neq 0) > 0$$
$$V(|x| \to \infty) \to \infty \quad (11)$$
$$\dot{V}(x \neq 0) < 0$$

Therefore, the stability condition is defined as:

$$V(x \neq 0)\dot{V}(x \neq 0) < 0 \quad (12)$$

Hence, it is necessary to define a positive definite candidate Lyapunov function (13).

$$V = k_I \frac{{e_I}^2}{2} + \frac{{e_u}^2}{2} \quad (13)$$

According to direct method of Lyapunov (discussed in the previous chapter), the time derivative of V must be negative. To guarantee that this condition is verified the virtual input current must obey $i_d = i_{dv}$ for $k_u > 0, \Rightarrow k_I > 0$.

$$\frac{dV}{dt} < 0 \Rightarrow k_I e_I \frac{de_I}{dt} + e_u = -k_u {e_u}^2 \quad (14)$$

From the (14):

$$k_I e_I e_u + e_u\left(\frac{du_{Ciref}}{dt} - \frac{du_{Ci}}{dt}\right) = -k_u {e_u}^2 \quad (15)$$

Providing:

$$k_I e_I + \left(\frac{du_{Ciref}}{dt} - \left(\frac{G_i}{C_i} i_{dv} + \frac{i_{dc}}{C_i}\right)\right) = -k_u e_u \quad (16)$$

Therefore, the virtual control action is the following:

$$i_{dv} = \frac{u_{Ci}}{u_{Gi}}\left(C_i\left(k_I e_I + k_u e_u + \frac{du_{Ciref}}{dt}\right) - i_{dc}\right) \quad (17)$$

Equation (17) is the Lyapunov equivalent of a PI controller, since the virtual control action i_{dv} depends on the e_u and on the integral e_I of the error e_u.

From (17) a nonlinear voltage controller is obtained. This controller will generate a i_{dq0ref} that will be used in the nonlinear current controller. However, the nonlinear current controller will work in $\alpha\beta$ coordinates hence, the i_{dq0ref} will be transformed in $i_{\alpha\beta}$ through the following transformation matrix [10]:

$$\begin{bmatrix} i_\alpha \\ i_\beta \\ i_0 \end{bmatrix} = \begin{bmatrix} \cos(\omega t) & -\sin(\omega t) & 0 \\ \sin(\omega t) & \cos(\omega t) & 0 \\ 0 & 0 & 1 \end{bmatrix} \begin{bmatrix} i_d \\ i_q \\ i_0 \end{bmatrix} \quad (18)$$

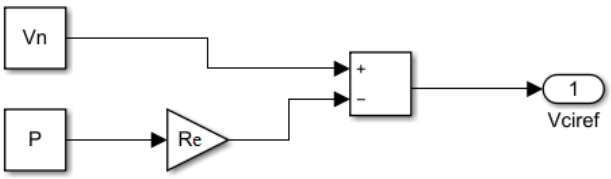

Figure 8 – Droop control representation

The V_{ciref} present in the Fig. 8 is express as follows:

$$V_{ciref} = V_n - R_e P \quad (19)$$

Where R_e represents the droop control. In this case the droop control is characterized by a voltage variation rate with the active power generated. The R_e units will be Volt per Watt.

2) Power Controller

For the sake of simplicity, the power controller will be design in dq coordinates. Hence, the measure voltage in abc coordinates will be transformed in dq coordinates by the transformation matrix present in (20) [10]. Thereby, it is possible to have a simpler control system, once instead of the three time-dependent signs the system will be composed by two continuous signals (V_d, V_q).

$$\begin{bmatrix} V_a \\ V_b \\ V_c \end{bmatrix} = \sqrt{\frac{2}{3}} \begin{bmatrix} \cos\theta & -\sin\theta & \frac{1}{\sqrt{2}} \\ \cos\left(\theta - \frac{2\pi}{3}\right) & -\sin\left(\theta - \frac{2\pi}{3}\right) & \frac{1}{\sqrt{2}} \\ \cos\left(\theta - \frac{4\pi}{3}\right) & -\sin\left(\theta - \frac{4\pi}{3}\right) & \frac{1}{\sqrt{2}} \end{bmatrix} \begin{bmatrix} V_d \\ V_q \\ V_0 \end{bmatrix} \quad (20)$$

Therefore, the active and reactive power in dq coordinates can be calculated as follows [11]:

$$\begin{cases} P = v_d i_d + v_q i_q \\ Q = v_q i_d - v_d i_q \end{cases} \quad (21)$$

After some mathematical manipulation, equation (21) can be solved for i_d, i_q, giving (22).

$$\begin{cases} i_d = \dfrac{P v_d + Q v_q}{{v_d}^2 + {v_q}^2} \\ i_q = \dfrac{P v_q - Q v_d}{{v_d}^2 + {v_q}^2} \end{cases} \quad (22)$$

The i_{dq} present in (22) will be used in the nonlinear current controller but in α, β coordinates, trough the transformation matrix (18).

3) Nonlinear Current Controller of the Inverter-Rectifier

Considering the Fig. 2, the AC currents dynamics is (23).

$$L\frac{di_k}{dt} = V_{kN} - Ri_K - e_k \; ; k \in \{A, B, C\} \quad (23)$$

Using α, β transformation, and denoting $i_{\alpha,\beta}$ for to represent both i_α, and i_β, it is possible to rewrite (23) as follows:

$$L\frac{di_{\alpha,\beta}}{dt} = V_{\alpha,\beta} - Ri_{\alpha,\beta} - e_{\alpha.\beta} \quad (24)$$

Using sliding mode control, the control objective can be defined in the following equation:

$$e_{i_{\alpha,\beta}} = i_{\alpha,\beta v} - i_{\alpha,\beta} = 0 \quad (25)$$

Therefore, the time-varying linear surface $s(x)$ is defined as:

$$s(x) = i_{\alpha,\beta v} - i_{\alpha,\beta} = e_{i_{\alpha,\beta}} \quad (26)$$

To enforce the sliding surface reaching after a finite time it is needed the use of the second method of Lyapunov as a stability condition. Hence, the candidate Lyapunov function can be express as:

$$V = \frac{1}{2}s^2 = \frac{{e_{i_{\alpha,\beta}}}^2}{2} \quad (27)$$

The stability condition according to Lyapunov is given by:

$$e_{i_{\alpha,\beta}}\frac{de_{i_{\alpha,\beta}}}{dt} < 0 \quad (28)$$

Thus, the control conditions can be express by:

$$\begin{cases} If\ e_{i_{\alpha,\beta}} > 0 \Rightarrow i_{\alpha,\beta} \uparrow \Rightarrow V_{\alpha,\beta} > Ri_{\alpha,\beta} + e_{\alpha,\beta} \\ If\ e_{i_{\alpha,\beta}} < 0 \Rightarrow i_{\alpha,\beta} \downarrow \Rightarrow V_{\alpha,\beta} < Ri_{\alpha,\beta} + e_{\alpha,\beta} \end{cases} \quad (29)$$

Where,

$$i_{\alpha,\beta} = i_{\alpha,\beta v} \pm \Delta i/2 \quad (30)$$

Considering (29) the reaching condition is given by:

$$V_{\alpha,\beta} > \left|Ri_{\alpha,\beta} + e_{\alpha.\beta}\right| \quad (31)$$

The objective of this control is to achieve a zero error between the reference value and the variables to control. This would imply an infinite switching frequency which is not possible, because the semiconductors have physical speed limitations. Hence, to circumvent this issue the error must be bounded. Therefore, the nonlinear current control based on sliding mode control theory will be given by the following conditions:

$$\begin{cases} If\ e_{i_{\alpha,\beta}} > +\dfrac{\Delta i}{2} \Rightarrow \delta_{\alpha,\beta} = 1 \\ If\ -\dfrac{\Delta i}{2} < e_{i_{\alpha,\beta}} < +\dfrac{\Delta i}{2} \Rightarrow \delta_{\alpha,\beta} = 0 \\ If\ e_{i_{\alpha,\beta}} < -\dfrac{\Delta i}{2} \Rightarrow \delta_{\alpha,\beta} = -1 \end{cases} \quad (32)$$

$$\begin{cases} i_{\alpha,\beta v} > i_{\alpha,\beta} \Rightarrow i_{\alpha,\beta} \uparrow \Rightarrow \dfrac{di_{\alpha,\beta}}{dt} > 0 \Rightarrow V_{\alpha,\beta} > 0 \\ i_{\alpha,\beta v} \approx i_{\alpha,\beta} \Rightarrow i_{\alpha,\beta} \uparrow\downarrow \Rightarrow \dfrac{di_{\alpha,\beta}}{dt} \approx 0 \Rightarrow V_{\alpha,\beta} = 0 \\ i_{\alpha,\beta v} < i_{\alpha,\beta} \Rightarrow i_{\alpha,\beta} \downarrow \Rightarrow \dfrac{di_{\alpha,\beta}}{dt} < 0 \Rightarrow V_{\alpha,\beta} < 0 \end{cases} \quad (33)$$

The i_α and i_β will provided by the i_{abc} currents transformed in to $\alpha\beta 0$ coordinates trough the following transformation matrix [10]:

$$\begin{bmatrix} i_\alpha \\ i_\beta \\ i_0 \end{bmatrix} = \begin{bmatrix} 1 & -\frac{1}{2} & -\frac{1}{2} \\ 0 & \frac{\sqrt{3}}{2} & -\frac{\sqrt{3}}{2} \\ \frac{1}{\sqrt{2}} & \frac{1}{\sqrt{2}} & \frac{1}{\sqrt{2}} \end{bmatrix} \begin{bmatrix} i_a \\ i_b \\ i_c \end{bmatrix} \quad (34)$$

B. DC-DC Converter Controllers

As said the multiterminal DC network contains constant power and constant current electronic loads. These electronic loads will be simulated using three-level DC-DC converters. To control current and voltage in the DC-DC converters similar nonlinear controllers used earlier will be applied. Therefore, in this section the combination between backstepping and sliding mode control will be the chosen method. First, the backstepping method is used to control voltage by defining a virtual control current, while a sliding mode current controller will be used to enforce the DC current to track the virtual current reference.

1) Nonlinear Voltage Controller of the DC-DC Converter

Appling the same principle of section III a), considering Fig. 3 the dynamic behaviour of the DC currents is the following:

$$\begin{cases} \dfrac{dv_c}{dt} = \dfrac{i_L - i_0}{C} \\ \dfrac{di_L}{dt} = \dfrac{V_i - V_0}{L} \end{cases} \quad (35)$$

In this case the control objective is defined as:

$$V_0 = V_{0ref} \tag{36}$$

Moreover, the error (e_{v_0}) between the reference voltage and the capacitor voltage is express as:

$$e_{V_0} = V_{0ref} - V_0 \tag{37}$$

The candidate Lyapunov function is defined as:

$$V_L = \frac{{e_{V_0}}^2}{2} \tag{38}$$

The Lyapunov function (38) must verified the (11) and (12) conditions to be asymptotically stable. Therefore, $V_L > 0\ \forall e_{V_0} \neq 0$ and $V_L \to \infty\ for\ \|t\| \to \infty$.

The candidate Lyapunov function time derivative must be a negative definite as was explained before (39).

$$\dot{V}_L = e_{V_0}\frac{de_{V_0}}{dt} = -K_V {e_{V_0}}^2\ \ , K_V > 0 \tag{39}$$

According to the second method of Lyapunov the global asymptotic stability is defined as:

$$\frac{de_{V_0}}{dt} = -K_V e_{V_0} \Rightarrow \frac{de_{V_0}}{dt} = \frac{de_{V_{0ref}}}{dt} - \frac{i_L - i_0}{C} \tag{40}$$

Where, $e_{V_0} \neq 0$, the $\frac{de_{V_0}}{dt}$ using (35) and (36) is defined as:

$$\frac{de_{V_0}}{dt} = -K_V e_{V_0} \Rightarrow \frac{de_{V_0}}{dt} = \frac{de_{V_{0ref}}}{dt} - \frac{i_L - i_0}{C} \tag{41}$$

Thus, replacing in the previous equation (41) i_L by i_{Lref} where, i_{Lref} is the virtual control variable, it is possible to control V_0 by defining i_{Lref}:

$$i_{Lref} = CK_V e_{V_0} + C\frac{de_{V_{0ref}}}{dt} + i_0 \tag{42}$$

2) Nonlinear Current Controller of the DC-DC Converter

To design the nonlinear current controller the same principle of section III b) will be applied, but in this case to a DC-DC converter [8].

Considering the Fig. 3 is possible to write the following dynamic equation:

$$L\frac{di_L}{dt} = V_i - V_0 \tag{43}$$

Considering equation (2) it is possible to rewrite equation (43) as follows:

$$\frac{di_L}{dt} = \frac{\gamma U - V_0}{L} \tag{44}$$

The control objective is given by the following equation:

$$e_{i_L} = i_{Lref} - i_L = 0 \tag{45}$$

Moreover, the time-varying linear surface $s(x)$ is defined as:

$$s(x) = i_{Lref} - i_L = e_{i_L} \tag{46}$$

To enforce that the sliding surface is reached after a finite period is needed the use of the second method of Lyapunov as a stability condition. Therefore, the candidate Lyapunov function can be express as:

$$V = \frac{1}{2}s^2 = \frac{{e_{i_L}}^2}{2} \tag{47}$$

The stability condition according to the direct method of Lyapunov is satisfied, if $s\dot{s} < 0$. Thus:

$$\begin{aligned} &If, e_{i_L} > \frac{\Delta i_L}{2} \Rightarrow i_L \uparrow \Rightarrow \gamma = 1 \quad If, \gamma U > V_0 \\ &If, -\frac{\Delta i_L}{2} < e_{i_L} < \frac{\Delta i_L}{2} \Rightarrow \gamma = 0 \\ &If, e_{i_L} < -\frac{\Delta i_L}{2} \Rightarrow i_L \downarrow \Rightarrow \gamma = -1 \end{aligned} \tag{48}$$

IV. RESULTS

The objectives of this chapter are 1) to simulate the nonlinear controllers, explained in the previous chapters in the context of the described network (chapter II) and III) to analyse the obtained results.

In order to do the simulation a model of the multiterminal HVDC network including the before mentioned controllers was created in MATLAB/Simulink. All the values used in the grid are described in the tables 1,2 and 3.

Table 1 – Simulation parameters of the inverter

Inverter									
$\boldsymbol{\omega_f}$ $[\boldsymbol{rad/s}]$	f $[Hz]$	S_{cc} $[MVA]$	R_1 $[\Omega]$	L_0 $[mH]$	R_2 $[\Omega]$	C_0 $[\mu F]$	R_3 $[m\Omega]$	L_1 $[mH]$	V_{nac} $[kV]$
$6000\boldsymbol{\pi}$	50	1500	0.4	9.2	108.8	0.5	1	2.4	66

Table 2 – Simulation parameters of the π line

$\boldsymbol{\pi}$ **Line**						
$\boldsymbol{r}$ $[\boldsymbol{k\Omega}]$	C_i $[\mu F]$	R_{dc} $[\Omega/km]$	L_{dc} $[mH/km]$	C_{dc} $[\mu F/km]$	d $[km]$	r_{PL} $[k\Omega]$
450	24.178	0.0205	0.352	0.233	220	2.757

Table 3 – Simulation parameters of the DC-DC converter

DC-DC Converter			
$\boldsymbol{V_n[kV]}$	$I_n[A]$	$C[\mu F]$	$L[mH]$
150	1088	3	17.5

At $t = 0s$, the converters and power lines shown in Fig. 1 are in steady state with nominal operating values, except when said otherwise. Moreover, to evaluate the performance of the four terminal HVDC grid under large variation of power, at $t = 0.1s$ two constant power loads are connected into the grid, (one in each independent network), each one of them with half of the nominal power. At $t = 0.1s$ two constant power loads are connected into the grid. All the simulations have the duration of 0.8s.

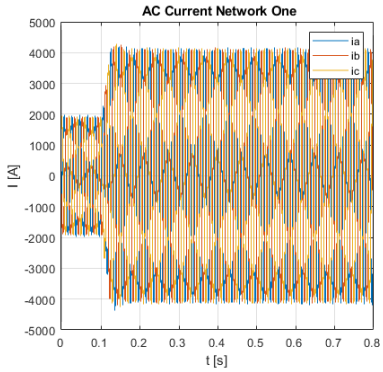

Figure 9 – Currents measured on the AC side of network one with nonlinear controller

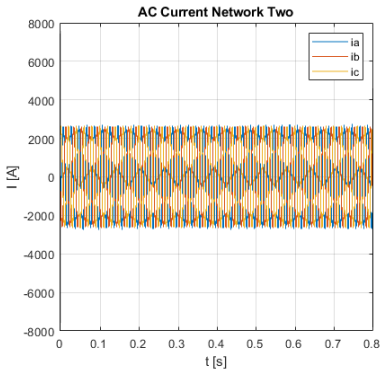

Figure 10 – Currents measured on the AC side of network two with nonlinear controller

In Fig. 9 it is possible to see the evolution of the AC currents over time in the network one. The currents at $t = 0s$ up to $t = 0.1s$ have the same Root Mean Square (RMS) value which is constant. After that, the currents have a big increase because at that time the constant power loads are connected to the grid, with the system power also increasing, so that RMS value of AC currents has to increase as well due to the response of the line voltage controllers that increase the virtual current to maintain the line voltage. The RMS value of AC currents presented in the Fig. 10 don't increase when the constant power loads are connected, because the network two is power controlled and the power reference has to be kept constant (for wind or solar applications). Therefore, the increase of power in the network two due to the electronic load has to be supplied by the interconnecting line two.

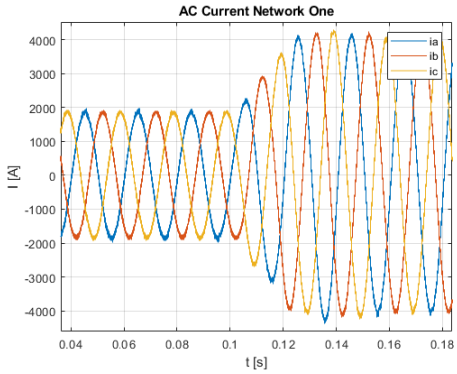

Figure 11 – Currents measured on the AC side of network one with nonlinear controller (zoom)

Fig. 11 presents a zoom in the AC currents waveform of network one to see their balanced sinusoidal behaviour.

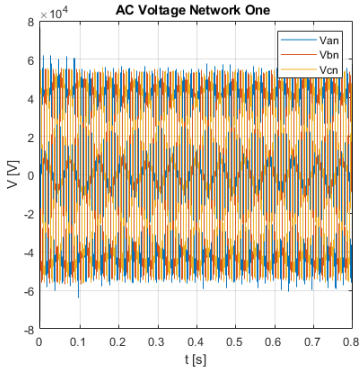

Figure 12 – Voltages measured on the AC side of network one with nonlinear controller

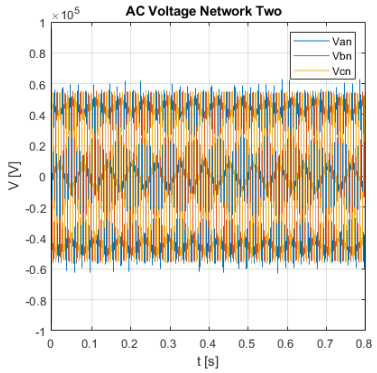

Figure 13 – Voltages measured on the AC side of network two with nonlinear controller

The evolution of the AC voltages in both networks, at the input of the LCL filter, as shown in figures 12 and 13, have constant RMS values over the simulation time and have the nearly the same peak value. This peak value is computed as follows:

$$V_{anpeak} = V_{bnpeak} = V_{cnpeak} = \frac{V_{nac}}{\sqrt{3}}\sqrt{2} \tag{49}$$

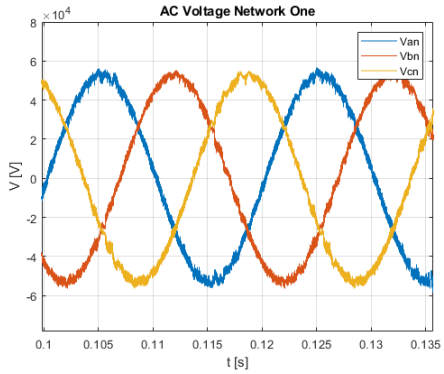

Figure 14 – Voltages measured on the AC side of network one with nonlinear controller (zoom)

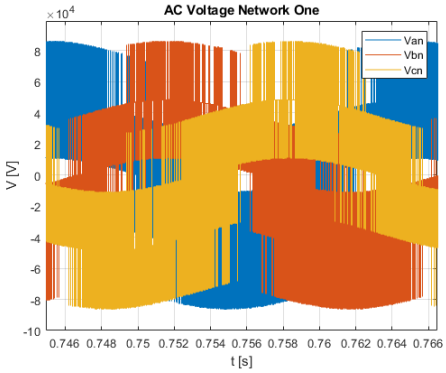

Figure 15 – Voltages measured on the AC side of network one with nonlinear controller without the LCL filter (zoom)

For a three-phase system to be balanced, all the source voltages must have the same magnitude and there must be exactly 120 degrees out of phase with one another, then it must be a 120-degree phase difference. Fig. 14 confirms that the AC source is a balanced three-phase system. The influence of the LCL filter is also shown in the same figure when compared with Fig. 15, because the waveform high frequency harmonics have highly reduced amplitude, otherwise the waveforms would show higher ripple.

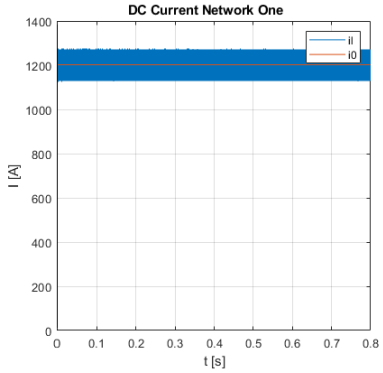

Figure 16 – Currents measured on the output DC side of network one with nonlinear controller

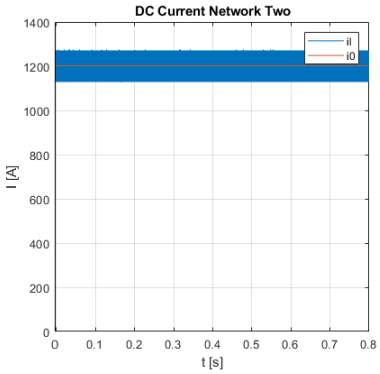

Figure 17 – Currents measured on the output DC side of network two with nonlinear controller

The output currents in the figures 16 and 17 have the same behaviour as expected, because the two networks have similar parameters and have the same type of controllers. The output current i_0 in both networks has average value equal to 1200A because the constant current load imposes that value. In other hand the ripple current in inductor L, i_L has a triangle waveform as expected. This behaviour is possible to see in Fig. 18.

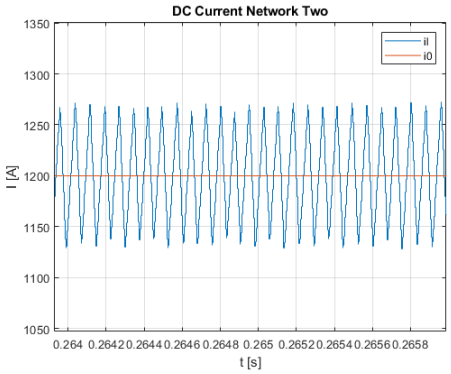

Figure 18 – Currents measured on the output DC side of network one with nonlinear controller (zoom)

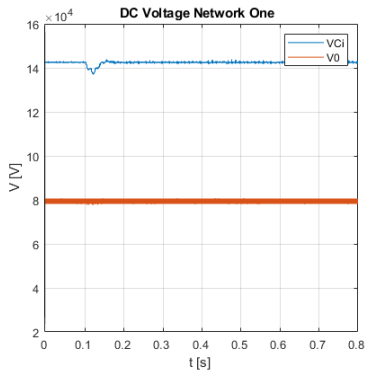

Figure 19 – Voltages measured on the DC side of network one with nonlinear controller

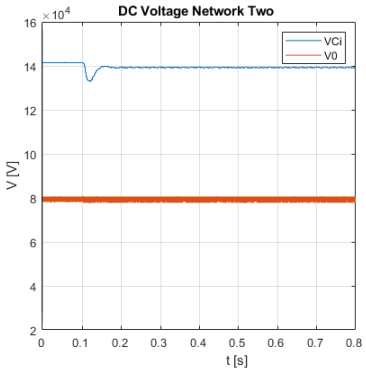

Figure 20 – Voltages measured on the DC side of network two with nonlinear controller

The V_{Ci} is the DC voltage at the DC side of the inverter-rectifier and the V_0 is the DC voltage at the output of the network, as shown in the Fig. 6. From figures 19 and 6.20 it is seen that the nonlinear controllers, at $t = 0.1s$, after a brief transient maintain the grid voltage in droop mode when the constant power loads are connected to the grid. Hence, the V_{ci} voltage droops, but after that the controller rises the voltage to a value slight lower than the rated value. However, in the network two (Fig. 20) the error is greater. This happens because in this network only the injected power is controlled not the line voltage. It is possible to minimize this error injecting more power, but in this case extra power, if available, is not strictly needed as the deviation from the rated voltage is not significant. In the network one the voltage drops 5.6 kV approximately; in the second network the voltage drops 8.6 kV (≈ -5%). In other hand, the electronic load voltage V_0 is always equal to 80 kV as expected, showing no voltage oscillations. Moreover, in the figures 21 and 22 is expressed the same test but without the droop control action. It is seen the line voltage returns to 150 kV not depending on that disturbance.

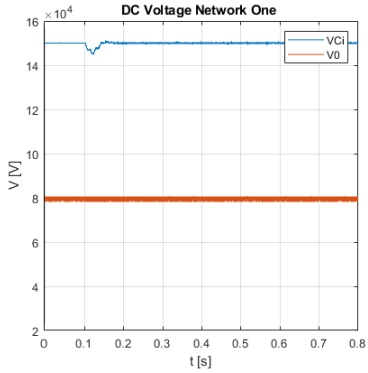

Figure 21 – Voltages measured on the DC side of network one with nonlinear controller without droop control

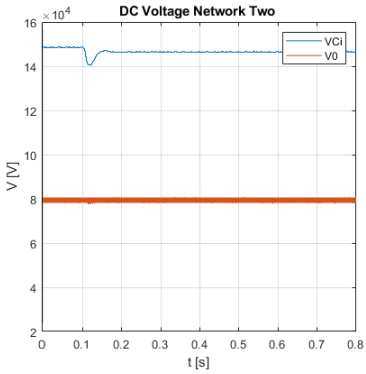

Figure 22 – Voltages measured on the DC side of network two with nonlinear controller without droop control

A. *THD Analysis*

The type of network discussed in this dissertation is supplied by high voltage in the AC side, where the total harmonic distortion (THD) must be smaller than 5%. Therefore, in this section a THD analysis is made to check if the THD in the multiterminal network presents acceptable values. To perform this analysis the FFT analysis tool of MATALAB/Simulink is used. All studies were made using a fundamental frequency of 50 Hz with while sampling 5 cycles.

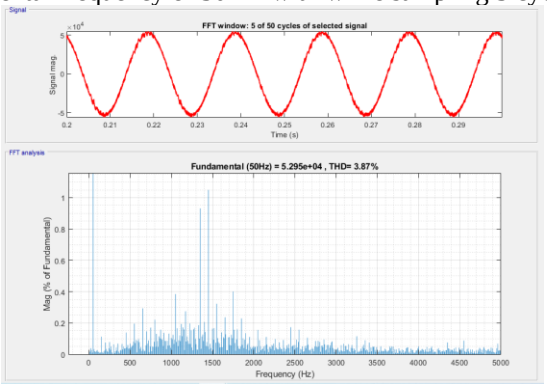

Figure 23 – AC Voltage FFT analysis network one using nonlinear controllers

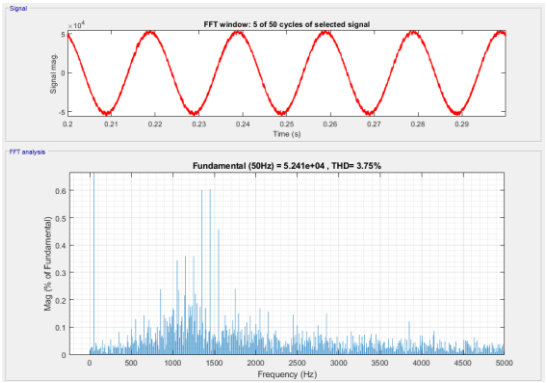

Figure 24 – AC Voltage FFT analysis network two using nonlinear controllers

From Fig. 23 it is concluded that the THD of the AC voltage in network one is less than 5% and equal to 3.87%. In the case of network two the THD of AC voltage it is also less than 5% and equal to 3.75% (Fig. 24).

The table 4 summarizes the above discussed AC voltages THD, while adding corresponding THD results for DC voltages. It can be seen that the DC voltage THDs are acceptably low.

Table 4 – THD values

	THD AC		**THD DC**	
	AC Voltages		V_{ci} Voltage	
	Network 1	Network 2	Network 1	Network 2
Nonlinear Control	3.87%	3.75%	0.199%	0.042%
Linear Control	3.87%	3.78%	0.256%	0.048%

V. CONCLUSIONS

This paper has developed nonlinear voltage controllers to implement in a four-terminal VSC-HVDC standard network. The standard multi-terminal DC network is composed by two similar networks that are interconnected by a third line. To model the multiterminal network, lines were represented by their π models, while each network constant power load, current constant load, AC/DC inverter-rectifier and DC/DC converters were modelled using their state-space equations. Due to the topology of the entire network and the presence of constant power loads, two different nonlinear control techniques were developed and implemented to ensure the global stability, overcoming the stability issue possibly caused by constant power loads in the HVDC network. To check the performance of nonlinear controllers, the steadiness of the DC voltage and their transient and dynamic response were evaluated when the constant power loads were connected.

The first nonlinear controller proposed in this dissertation is based on Lyapunov control theory and combines backstepping control with sliding mode control. These controllers coupled to LCL filters, to attenuate high frequency harmonics, have shown good performance with voltage variations less than 5% and THD less than 4%.

The second nonlinear controller presented in this dissertation is also based on Lyapunov theory but in this case, it is adapted to DC-DC converters. This controller has shown a good performance in terms of stability and response speed to attain the steady state after the disturbances.

In this dissertation results were obtained with and without droop control. The usual solution for this type of application is the use of droop control. Thus, the reference voltage is dependent on the required active power, which enables a better result in terms of stability because in the multiterminal network power and voltage are controlled.

The AC voltage THD of network one is equal to 3.87% and equal to 3.75% on network two. The DC voltage THDs are acceptably low and it can be seen that the THDs using nonlinear control are lower than using linear control. Therefore, all THD are small (less than 5 %).

VI. REFERENCES

[1] D. J. Becker and B. J. Sonnenberg, "400Vdc power distribution: Overcoming the challenges," *INTELEC, Int. Telecommun. Energy Conf.*, 2010, doi: 10.1109/INTLEC.2010.5525660.

[2] F. D. Bianchi and O. Gomis-Bellmunt, "Droop control design for multi-terminal VSC-HVDC grids based on LMI optimization," *Proc. IEEE Conf. Decis. Control*, pp. 4823–4828, 2011, doi: 10.1109/CDC.2011.6161070.

[3] M. S. Carmeli, D. Forlani, S. Grillo, R. Pinetti, E. Ragaini, and E. Tironi, "A stabilization method for DC networks with constant-power loads," *2012 IEEE Int. Energy Conf. Exhib. ENERGYCON 2012*, pp. 617–622, 2012, doi: 10.1109/EnergyCon.2012.6348226.

[4] H. Wang and M. A. Redfern, "The advantages and disadvantages of using HVDC to interconnect AC networks," *Proc. Univ. Power Eng. Conf.*, pp. 4–8, 2010.

[5] R. A. F. Ferreira, P. G. Barbosa, H. A. C. Braga, and A. A. Ferreira, "Analysis of non-linear adaptive voltage droop control method applied to a grid connected DC microgrid," *2013 Brazilian Power Electron. Conf. COBEP 2013 - Proc.*, pp. 1067–1074, 2013, doi: 10.1109/COBEP.2013.6785247.

[6] Luís Nunes, Master Thesis: "Voltage Nonlinear Control in Multiterminal HVDC Networks",2020

[7] E. Hossain, R. Perez, A. Nasiri, and S. Padmanaban, "A Comprehensive Review on Constant Power Loads Compensation Techniques," *IEEE Access*, vol. 6, pp. 33285–33305, 2018, doi: 10.1109/ACCESS.2018.2849065.

[8] J. F. Silva, 'Electrónica Industrial Semicondutores e Conversores de Potência, série Manuais Universitários,' Lisboa, Fundação Calouste Gulbenkian, 2013." .

[9] J. Huang, D. Xu, W. Yan, L. Ge, and X. Yuan, "Nonlinear Control of Back-to-Back VSC-HVDC System via Command-Filter Backstepping," *J. Control Sci. Eng.*, vol. 2017, 2017, doi: 10.1155/2017/7410392.

[10] G. Marques, "Dinâmica das Máquinas Eléctricas," p. 289, 2002.

[11] F. Silva, S. Pinto, and J. Santana, "Conversores Comutados para Energias Renováveis," p. 172, 2016, [Online]. Available: https://fenix.tecnico.ulisboa.pt/downloadFile/563568428750567/Livro_CCER_2017.pdf.